AFRL-MN-EG-TR-1998-7092

ANALYSIS OF CORRELATION FILTERS FOR OPEL

David L. Flannery

University of Dayton Research Institute
Electrical and Computer Engineering Division
300 College Park
Dayton OH 45469-0150

September 1998

FINAL REPORT FOR PERIOD APRIL 1997 - JULY 1998

19981125 016

AIR FORCE RESEARCH LABORATORY, MUNITIONS DIRECTORATE
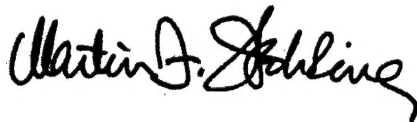**Air Force Materiel Command ■ United States Air Force ■ Eglin Air Force Base**

DTIC QUALITY INSPECTED 3

NOTICE

When Government drawings, specifications, or other data are used for any purpose other than in connection with a definitely Government-related procurement, the United States Government incurs no responsibility or any obligation whatsoever. The fact that the Government may have formulated or in any way supplied the said drawings, specifications, or other data, is not to be regarded by implication, or otherwise as in any manner construed, as licensing the holder, or any other person or corporation; or as conveying any rights or permission to manufacture, use, or sell any patented invention that may in any way be related thereto.

This technical report has been reviewed and is approved for publication.

FOR THE COMMANDER

MARTIN F. WEHLING
Technical Director, Advanced Guidance Division

Even though this report may contain special release rights held by the controlling office, please do not request copies from the Air Force Research Laboratory, Munitions Directorate. If you qualify as a recipient, release approval will be obtained from the originating activity by DTIC. Address your request for additional copies to:

Defense Technical Information Center
8725 John J. Kingman Road, Ste 0944
Ft Belvoir VA 22060-6218

If your address has changed, if you wish to be removed from our mailing list, or if your organization no longer employs the addressee, please notify AFRL/MNGI, Eglin AFB FL 32542-6810, to help us maintain a current mailing list.

Do not return copies of this report unless contractual obligations or notice on a specific document requires that it be returned.

REPORT DOCUMENTATION PAGE

Public reporting burden for this collection of information is estimated to average 1 hour per response, including the time for reviewing instructions, searching existing data sources, gathering and maintaining the data needed, and completing and reviewing the collection of information. Send comments regarding this burden estimate or any other aspect of this collection of information, including suggestions for reducing this burden, to Washington Headquarters Services, Directorate for Information Operations and Reports, 1215 Jefferson Davis Highway, Suite 1204, Arlington, VA 22202-4302, and to the Office of Management and Budget, Paperwork Reduction Project (0704-0188), Washington, DC 20503.

1. AGENCY USE ONLY *(Leave blank)*	2. REPORT DATE September 1998	3. REPORT TYPE AND DATES COVERED Final Technical Report Apr 97 – Jul 98

4. TITLE AND SUBTITLE Analysis of Correlation Filters for OPEL	5. FUNDING NUMBERS Grant #: F08630-97-1-0004 JON: 20683002 PE: 62602F PR: 2068 TA: 30 WU: 02
6. AUTHOR(S) David L. Flannery	

7. PERFORMING ORGANIZATION NAME(S) AND ADDRESS(ES) University of Dayton Research Institute Electrical and Computer Engineering Division 300 College Park Dayton OH 45469-0150	8. PERFORMING ORGANIZATION REPORT NUMBER UDR-TR-1998-00090

9. SPONSORING/MONITORING AGENCY NAME(S) AND ADDRESS(ES) (Program Mgr Name & Ph #) Air Force Research Laboratory Munitions Directorate Seeker Image and Signal Processing Branch 101 W Eglin Blvd Suite 280 Eglin AFB FL 32542-6810 Program Manager: Dr. Dennis H. Goldstein AFRL/MNGI/PH: 850-882-4636	10. SPONSORING/MONITORING AGENCY REPORT NUMBER AFRL-MN-EG-TR-1998-7092

11. SUPPLEMENTARY NOTES

12a. DISTRIBUTION/AVAILABILITY STATEMENT Unlimited Distribution - Approved for Public Release	12b. DISTRIBUTION CODE

13. ABSTRACT:

Correlation filter design and image preprocessing techniques applicable to ladar images from the Optical Processor Enhanced Ladar (OPEL) program (see AFRL-MN-EG-TR-1998-7095) were investigated under this grant. Government-furnished mask images were used for most of the study. Range-operator edge enhancement followed by thresholding and dilation were found to be the best preprocessing combination to generate binary correlator input images. Parametric correlation simulation studies explored the variation of correlation performance with filter azimuth coverage. Smart filters were based on the iterated-LASE formulation. An algorithm for direct processing of range image files to yield binary correlator input images containing both outline and internal detail was developed.

14. SUBJECT TERM Optical Correlator, Correlation Filter			15. NUMBER OF PAGES 26
			16. PRICE CODE

17. SECURITY CLASSIFICATION OF REPORT Unclassified	18. SECURITY CLASSIFICATION OF THIS PAGE Unclassified	19. SECURITY CLASSIFICATION OF ABSTRACT Unclassified	20. LIMITATION OF ABSTRACT SAR

NSN 7540-01-280-5500

PREFACE

This is the final technical report for an effort performed by the University of Dayton Research Institute under Grant F08630-97-1-1004 for the Air Force Research Laboratory Munitions Directorate (AFRL/MNGI), Eglin AFB, Florida. The reported effort involved analysis and simulation of image preprocessing, correlation filter construction, and correlation performance for ladar images in support of the Optical Processor Enhanced Ladar (OPEL) program. It was performed in the Electrical and Computer Engineering Division of the Research Institute. The principal investigator was Dr. David L. Flannery and the effort was performed over the period from April 1997 through July 1998. The Air Force project manager was Dr. Dennis H. Goldstein of AFRL/MNGI.

TO BE LEFT BLANK

Table of Contents

TO BE LEFT BLANK

ANALYSIS OF CORRELATION FILTERS FOR OPEL

1.0 INTRODUCTION

The investigation reported herein included analysis and simulation of image preprocessing, correlation filter design, and digital simulations of correlator performance applicable to the Optical Processor Enhanced Ladar (OPEL) program.

Preprocessing techniques for generating binary correlator input images, and the design and optimization of distortion-invariant ("smart") binary phase-only correlation filters, were investigated. A small portion of the effort addressed direct processing of ladar range images with the goal of enhancing internal target detail not present in the "mask" images furnished by the sponsor.

The effort used Government-furnished binary image sets for M48 and M60 tank targets covering 0° - 180° azimuth in 0.27° steps and elevations of 22°, 25° and 28°.

Section 2 provides a summary of the effort and its results. Section 3 presents the preprocessing methods. Section 4 discusses the filter optimization studies. Section 5 reports the direct-range processing investigation. A filter-input set generated for use in determining simulation-vs.-experimental correlation intensity calibrations is described in Section 6. Section 7 provides concluding remarks and recommendations for further study.

2.0 SUMMARY OF THE EFFORT

This section presents a brief summary of the areas investigated and the results achieved. Subsequent sections discuss the effort in detail.

2.1 Preprocessing of Mask Images

Binary mask images derived from ladar tower test images were furnished by the Government sponsor. Preprocessing options were selected to be edge enhancement with range and Sobel operators, dilation, and thresholding. These were all investigated to optimize correlation performance. Smart filters covering 4° degrees azimuth and all three elevations were generated based on each preprocessing variant and were tested over the range of input images spanning the filter coverage. The iterated least-aggregate square error (ILASE) filter formulation was used. Average peak response, response uniformity over the designed distortion range, and rejection of targets outside the design azimuth range were evaluated in correlation simulations.

Based on the simulation results, the optimum preprocessing sequence was determined to be 5x5 range edge enhancement followed by a two-pixel dilation (see Section 4.3).

2.2 Optimum Filter Design

The filter design goal is to find the combination of filter design parameters that optimizes overall filter performance. This involves maximizing the distortion coverage (azimuth, elevation, etc.) while achieving sufficient correlation peak intensities for detection above clutter and noise and adequate discrimination of other targets (e.g., M48 vs. M60). Design parameters include the threshold line angle (TLA), distortion parameter ranges (e.g., 4°,6°, 8° or 12° of azimuth), and training image intervals (e.g., 1° or 2° azimuth steps).

Designs were constrained to binary phase-only filters (BPOF), and the ILASE (iterated least aggregate square error) filter formulation (see Section 4.1) was used.

Filter optimization was conducted by extensive filter construction and correlation simulation testing, exploring parametric variations of the design variables. From these studies it was concluded that 8° azimuth coverage (with coverage of 22°, 25° and 28° elevations) is the maximum that can be recommended. The primary limiting factor is azimuth selectivity which degrades as filter coverage is increased, as would be expected (See Section 4.4).

2.3 Direct Range Preprocessing

Software was generated to process the "raw" range image files, which have 16-bit integer range values for each pixel. A height image was computed, preprocessed for noise reduction, and thresholded to remove all responses from objects other than the target (which was the highest object in the image). The output file was a standard 8-bit pixel image which readily could be further processed.

Various types of edge-enhancement and thresholding operations were investigated with the goal of suppressing fixed and impulse noise while rendering internal target details visible. A combination was found that yielded promising results based on visual inspection.

2.4 Intensity Calibration

A set of input images and a filter were generated as a test set for insertion into the experimental correlator for the purpose of determining the minimum correlation peak design value required in filter design computations. (See Section 6 for details.)

2.5 Conclusions and Recommendations

The reader is referred to Section 7 for concluding remarks and recommendations for further study.

2

3.0 Preprocessing of Mask Images

The left image in Figure 3.1 is an example of a binary ladar mask image as furnished.
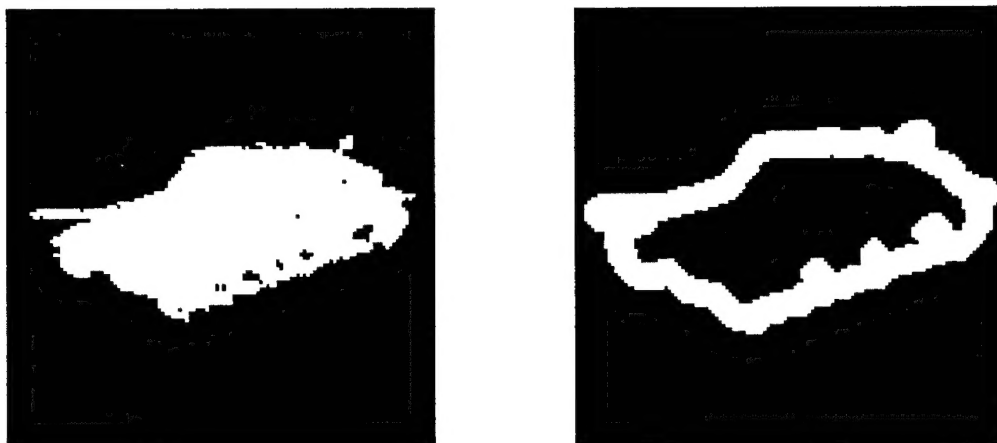

Figure 3.1 Examples of mask (left) and preprocessed (right) images.

The right image in the same figure is the result of applying the preprocessing steps found to be optimum in this study (See Section 4.3). In general, optical correlation selectivity or discrimination is improved by using edge images, although it is also recognized that phase-only filters (as used in this effort) have an intrinsic edge enhancement property.

Several well-known edge-enhancement operators, plus dilation and thresholding steps were combined in a correlation simulation study to investigate the relative merits of such techniques for correlation using binary inputs and binary phase-only filters (BPOF). This section briefly describes the algorithms. Details of the study and its results may be found in Section 4.

3.1 Edge enhancement operators

Edge enhancement convolution operators used in the study included the range and Sobel operations[1].

Range operators replace each pixel value with the difference between maximum and minimum pixel values (the range) taken over a region centered on the pixel. The size of the region (e.g., 3x3 or 5x5) defines variants of the range operator. Advantages of this operator include that it is approximately omnidirectional and that it produces a unipolar (positive or zero) response.

The 3x3 Sobel operators are well known. They are directional and are usually applied in orthogonal pairs. They produce a bipolar (positive, zero, or negative) response. In this study the horizontal and vertical pair were applied. The absolute

values of the two responses were added at each pixel and normalized by a constant to prevent overflow. There are other options for combining two orthogonal Sobel results to obtain a single positive value representing edge strength [1]. The one used here is as good as any and requires less computation than, for example, taking the RMS value of the orthogonal values.

3.2 Thresholding

Ultimately, a preprocessed image must be thresholded to produce a binary image for the input plane of the correlator. In the case of range processing of the furnished mask images, thresholding is not required because the range operator applied to a binary image generates a binary output image. For other cases, a spatially constant threshold was automatically computed based on the image histogram. The threshold value is chosen to "turn on" (set to the non-zero binary value) an operator-specified fraction of the nonzero image values. Typical threshold settings that produce good correlation images turn on 40% to 60% of the nonzero pixels. Exclusion of the zero-valued pixels from the histogram computation is a convenience when the image has a large background of zero pixel values. With this approach the optimum value for correlation tends to stay near 50% as the area ratio of target to background varies widely.

3.3 Dilation

The dilation operation [1] applied to a binary image causes each neighboring pixel of any nonzero pixel to also be set to the nonzero state in the output image. The definition of 'neighboring' always includes the vertically and horizontally connected north-south-east-west (NSEW) pixels but may or may not include the diagonally connected pixels.

Euclidean distance maps (EDMs) [1] provide an attractive method to compute multiple dilations while also addressing the issue of diagonal connectivity on a rational basis. In the EDM, each pixel value represents the minimum distance via any path (including those containing diagonal steps) to the nonzero portion of the original binary image. Thresholding the EDM at a chosen distance value provides a binary output image representing dilation by a number of pixels corresponding to the chosen threshold. The EDM can be constructed recursively with each step adding a layer to the previous EDM. Ideally, diagonal steps would be assigned a distance of 1.414.. ($\sqrt{2}$) times the distance of a NSEW step. However, it is computationally desirable to restrict the EDM to integer values. Thus the compromise value of 1.5 is frequently assigned to diagonal steps, as was done in this effort. Then NSEW steps are counted as two distance units and diagonal steps are counted as three distance units.

In this effort, two cycles of Euclidean dilation were performed and the result was thresholded to exclude pixels greater than four distance units (equal to two NSEW steps) . Thus pixels within either two NSEW steps or one diagonal step of the

4

original nonzero portion of the image were set to nonzero in the output image. This is at least roughly equivalent to combining two dilation steps, only one of which treats diagonally connected pixels as neighbors.

4.0 Optimum Filter Design

The filter design goal is to find the combination of filter design parameters that optimizes overall filter performance. This involves maximizing the distortion coverage (azimuth, elevation, etc.) while achieving sufficient correlation peak intensities for detection above clutter and noise and adequate discrimination of other targets (e.g., M48 vs. M60). Design parameters include the threshold line angle (TLA), distortion parameter ranges (e.g., 4°,6°, 8° or 12° of azimuth) and training image intervals (e.g., 1° or 2° azimuth steps).

Designs were constrained to binary phase-only filters (BPOF), and the ILASE (iterated least aggregate square error) filter formulation was used.

Filter optimization was conducted by extensive filter construction and correlation simulation testing while parametric variations of the design variables were explored.

4.1 The iterated-LASE filter formulation

The LASE (least aggregate square error, [2]) filter formulation meets the following defining goal:

Find the single filter, subject to constrained modulation, that minimizes the aggregate square-error in the correlation functions over a set of N test images consisting of a set of N training images with additive random noise described by a known power spectral density. The "error" is defined as the difference in (complex) correlation amplitude between correlations of a particular input with a filter optimized solely for that input and with the single LASE filter. The individual optimized filters may be optimized in any desired manner. The aggregate square-error is the magnitude-squared of this difference summed over the entire correlation plane and over the set of test images. In different words, the LASE filter is the single compromise filter that most closely approaches the performance of the N individual filters in a mean-square error sense, for additive random input noise of a given power spectral density. The defining publication [2] relates the LASE formulation to other published formulations and discusses how the aggregate square error of the filter can vary depending on degeneracies implicit in the optimization of the individual optimized filters. These details are beyond the scope of this report and the reader is referred to the cited reference for further discussion.

The mathematical expression for the LASE filter is:

$$H_{LASE,k} = \text{MED} \left\{ \frac{\sum_{n=1}^{N} H_{n,k} |T_{n,k}|^2}{\sum_{n=1}^{N} |T_{n,k}|^2} \right\} ,$$

where $H_{LASE,k}$ is the LASE filter function value for the k'th spatial frequency, MED denotes a minimum-Euclidean-distance mapping operation, $H_{n,k}$ is the n'th individual optimized filter value for the k'th spatial frequency, and $|T_{n,k}|^2$ is the power spectrum of the n'th test image. The MED operation outputs the modulation value on the locus of realizable filter modulation in the complex plane that is closest to the argument value.

Note that the LASE formulation is not inherently iterative, which leads to a computation-time advantage over the Jared-and-Ennis formulation [6] that was used in the DARPA TOPS program [7]. The Jared-and-Ennis formulation forms a filter based on a weighted composite of reference images. The Fourier transform of the composite image is thresholded to form a BPOF. Then iterations are performed in which the composite weights are adjusted relative to one another until the correlation response across the training set is uniform within an acceptable tolerance. The TOPS program used this type of smart filter in successful field tests in which tower-based and helicopter-based correlation systems recognized and located tanks based on real-time video images. The tanks were situated on a field test range at the U.S. Army Redstone Arsenal, and they were surrounded by other vehicles serving as clutter.

In this effort, the modulation constraint was binary-phase modulation. The individual optimized filters were BPOFs based on the binarized training images with a TLA (threshold line angle, [4]) that was known empirically to be near-optimum in terms of overall filter performance. Training image power spectra are the sum of the power spectrum of each training image and an estimated background-noise power spectral density. The background-noise power spectrum estimates may be formed based on representative scenes. However for the cases reported herein, the background-noise spectrum was assumed to be zero; i.e., the test images were identically the training images.

For BPOF filters, the MED operation to form the LASE filter is simply a thresholding of the argument value (which is pure real in this case) at zero to set 1 or -1 filter values.

The LASE formulation does not apply constraints in order to force or encourage response uniformity over the training set. It is usually desirable to improve the response uniformity of LASE filters. The LASE filter formulation algorithm has been augmented to incorporate iterative procedures for this purpose yielding the iterated-LASE (ILASE) formulation.

The formulation is modified by introducing real relative weighting coefficients, c_n, as follows:

$$H_{LASE,k} = \text{MED}\left\{\frac{\sum\limits_{n=1}^{N} c_n H_{n,k} \left|T_{n,k}\right|^2}{\sum\limits_{n=1}^{N} \left|T_{n,k}\right|^2}\right\}.$$

For phase-only filters, including the BPOF of concern herein, only the relative values of the c_n matter since multiplying all of them by a (real, non-zero) constant cannot change the resulting filter values other than to cause a trivial polarity reversal of all filter elements (which has no effect on detected correlation intensity).

The ILASE formulation builds an initial LASE filter with uniform weights (equal to unity). Then the central correlation intensity of each training image for the current filter is evaluated and the relative weighting of each image is adjusted up or down according to whether its relative BPOF-normalized correlation response is less than or greater than the average BPOF-normalized correlation response over the training set. This adjustment cycle is repeated until termination conditions (e.g., a desired uniformity) are met.

This relaxation algorithm is very similar to the one first proposed by Jared and Ennis [6] for improving response uniformity of composite phase-only filters across a training set. Note however that the LASE filter formulation, with or without the relative weighting concept, is fundamentally different from a composite filter, as discussed in the defining publication [2].

4.2 Filter design and correlation simulation details

The correlator hardware being simulated has a 256x256-pixel input spatial light modulator (SLM) effecting binary phase-only modulation. The filter SLM also implements binary phase-only modulation but has a 128x128-pixel format. Training and input digital images are in 256x256-pixel format.

The discrete Fourier transforms (DFT) used during filter formulation were performed with 256x256-samples and then averaged down (with 2x2 cell averages) to 128x128 formats, which were used to compute the desired 128x128-sample filter. During correlation simulations, the filters were "blocked up" (each sample was expanded to a 2x2 sub-array of samples having the original sample value), to provide a 256x256-sample array needed to multiply the DFT of the input image. This is a reasonable emulation of the situation realized in the optical correlator, in which the Fourier pattern is scaled to fit the 128x128-pixel active area of the filter SLM.

4.3 Preprocessing Optimization

A nearly head-on view of the M48 tank was chosen for initial preprocessing studies. Filters covering 4° through 8° azimuth were constructed using training intervals of one degree. All three available elevations were trained, as well as tilts (in-plane

rotations) of ±2°. No scale variations were trained as it is expected that the range to target will be known very accurately.

The filters are trained using only about one fourth of the mask images within the azimuth training range, since the mask images were captured at about 0.27° intervals. Correlation simulation testing was conducted using all the images in the in-band azimuth range, as well as all the images in an ex-band range centered 12° off the in-band range, i.e., 16° through 20° azimuth.

A number of different combinations of preprocessing steps were investigated. A 'standard' or baseline choice was 5x5 range algorithm preprocessing alone. The effect of varying filter TLA [4] was studied initially. Past experience indicates that TLA=30° is near optimum for targets such as those studied here which have mixtures of odd and even symmetry. Thus, TLA = 30 was added to the 'standard' case definition.

The following table summarizes the preprocessing and TLA study results. The 'case' column assumes the standard case except for the variation entered in the column.

Table 4.1 Preprocessing and TLA study results

Case	In-band Peak (intensity units)			Ripple	Ex-band rejection (dB)	
	Average	Min	Max	(%)	Average	Worst Case
TLA=0	8.44	6.25	10.68	52%	3.3	0.65
TLA=15	8.37	6.27	10.34	49%	3.5	0.74
TLA=30 (Std.)	7.94	5.75	9.69	50%	3.3	0.21
TLA=45	7.38	6.32	8.65	32%	3.2	0.96
Range 3x3	5.86	4.41	7.10	46%	3.7	0.60
Sobel 50%	5.10	3.67	6.05	47%	4.4	2.18
Sobel 75%	6.04	3.92	7.43	58%	4.1	0.41
5x5 Range, Dilated	11.26	8.58	13.18	41%	4.4	1.73

The percentage values included in the Sobel case names indicate the percentage of pixels turned on by the binarization threshold. The 'ripple' is the difference between maximum and minimum in-band peak intensity normalized to the average in-band intensity and expressed as a percentage. Ex-band rejection is the ratio of a

response (peak intensity) in the defined ex-band to an in-band response, expressed in decibels, i.e., 10 Log(intensity ratio). For average rejection, the average peak responses for the two bands are used. The worst case rejection figure is based on the greatest ex-band response and the smallest in-band response.

The TLA study is represented by the first three data lines in the table. The variations are small and to some degree erratic, and one could question the choice of 30° as optimum. However the impact of this choice is probably minor given the slow variation of the results with TLA.

The Sobel cases offer greater average ex-band rejection (i.e., discrimination) at the expense of lower average peak values (i.e., lower correlation efficiency). The greater computational demands of Sobel operators, compared with the range operators, are a disadvantage that must be considered.

The 5x5 range followed by dilation provides obviously superior average peak response, the second best ripple of the group and ex-band rejection equal to the best of the group. Thus it was judged superior on an overall basis and was used for all subsequent studies. Figure 3.1 provides an example of applying this preprocessing combination to a typical mask image.

4.4 Distortion range studies

4.4.1 Intended-target Performance

The intended-target performance results for the M48 and M60 filters and inputs at rear quartering view (135 degree nominal azimuth) using 4°,6°,8° and 12° azimuth coverage in the filters are summarized in the following four tables:

Table 4.2 Filter performance on intended targets with 4° azimuth coverage per filter, at 135° nominal azimuth (rear quartering view).

Target:	M48	M60
Average in-band response (intensity units):	11.92	13.59
Percent in-band ripple:	41.4%	46.5%
Average out-of-band discrimination (dB):	4.03	3.91
Worst case out-of-band discrimination (dB):	1.38	0.87
Correlations included in statistics:	47	45

9

Table 4.3 Filter performance on intended targets with 6° azimuth coverage per filter, at 135° nominal azimuth (rear quartering view).

Target:	M48	M60
Average in-band response (intensity units):	10.65	12.87
Percent in-band ripple:	51.6%	48.5%
Average out-of-band discrimination (dB):	3.73	3.62
Worst case out-of-band discrimination (dB):	0.83	0.46
Correlations included in statistics:	67	69

Table 4.4 Filter performance on intended targets with 8° azimuth coverage per filter, at 135° nominal azimuth (rear quartering view).

Target:	M48	M60
Average in-band response (intensity units):	10.65	12.05
Percent in-band ripple:	46.0%	48.4%
Average out-of-band discrimination (dB):	3.39	3.20
Worst case out-of-band discrimination (dB):	0.80	0.02
Correlations included in statistics:	91	92

Table 4.5 Filter performance on intended targets with 12° azimuth coverage per filter, at 135° nominal azimuth (rear quartering view).

Target:	M48	M60
Average in-band response (intensity units):	9.59	10.30
Percent in-band ripple:	53.1%	63.8%
Average out-of-band discrimination (dB):	2.77	2.17
Worst case out-of-band discrimination (dB):	-0.65	-1.18
Correlations included in statistics:	132	133

Similar studies also were carried out at broadside (nominal 90° azimuth) and frontal (6° central azimuth) aspects. The results follow.

Table 4.6 Filter performance on intended targets with 4° azimuth coverage per filter, at 90° nominal azimuth (broadside view).

Target:	M48	M60
Average in-band response (intensity units):	10.74	12.17
Percent in-band ripple:	43.0%	37.8%
Average out-of-band discrimination (dB):	3.34	2.53
Worst case out-of-band discrimination (dB):	1.10	0.37
Correlations included in statistics:	47	48

Table 4.7 Filter performance on intended targets with 8° azimuth coverage per filter, at 90° nominal azimuth (broadside view).

Target:	M48	M60
Average in-band response (intensity units):	10.53	10.99
Percent in-band ripple:	53.7%	37.3%
Average out-of-band discrimination (dB):	3.37	2.00
Worst case out-of-band discrimination (dB):	0.28	0.04
Correlations included in statistics:	90	88

Table 4.8 Filter performance on intended targets with 12° azimuth coverage per filter, at 90° nominal azimuth (broadside view).

Target:	M48	M60
Average in-band response (intensity units):	8.39	10.45
Percent in-band ripple:	65.7%	47.6%
Average out-of-band discrimination (dB):	*	*
Worst case out-of-band discrimination (dB):	*	*
Correlations included in statistics:	132	134

(*) Ex-band correlations were not performed for this simulation series.

Table 4.9 Filter performance on intended targets with 4° azimuth coverage per filter, at 6° nominal azimuth (frontal view). M60 images not available.

Target:	M48
Average in-band response (intensity units):	11.26
Percent in-band ripple:	40.9%
Average out-of-band discrimination (dB):	4.41
Worst case out-of-band discrimination (dB):	1.73
Correlations included in statistics:	49

4.4.2 Inter-target Discrimination

Given two targets, 'a' and 'b', and a filter that matches, for example, 'b', a discrimination ratio metric may be defined:

$$D_{ab} \equiv \frac{C_{bb}}{C_{ab}}$$

where C_{ab} denotes the peak correlation intensity when input 'a' is correlated with filter 'b'. The ratio as defined gives a greater value for better discrimination. Such ratios will be evaluated in decibels herein, i.e., ten times the logarithm of the ratio.

This ratio would apply if filters were only available for one target ('b' above). If filters are available for two targets ('a' and 'b') and it is assumed that the input is either 'a' or 'b' then a two-filter discrimination ratio may be defined:

$$D_{ab}^2 \equiv D_{ab} \Big/ D_{ba} \equiv \frac{C_{aa}}{C_{ab}} \cdot \frac{C_{ba}}{C_{bb}} \quad .$$

A further refinement is to use averages over the target distortion range corresponding to the smart filter design range for the auto-correlation terms in the above ratios, i.e.:

$$C_{aa} \Rightarrow \langle C_{aa} \rangle \quad \text{and} \quad C_{bb} \Rightarrow \langle C_{bb} \rangle .$$

Thus the cross-correlations are normalized to the average in-band response, i.e.,

$$C_{xb}^n \equiv \frac{C_{xb}}{\langle C_{bb} \rangle}$$

is the normalized correlation of input 'x' with the smart filter for target 'b'. It is trivially verified that if 'x' is in fact a 'b' target, the expected value of C_{xb}^n is unity. Thus the two types of discrimination ratio may be recast as:

$$D_{ab} \equiv \frac{1}{C_{ab}^n} \quad \text{and} \quad D_{ab}^2 \equiv \frac{C_{ba}^n}{C_{ab}^n}$$

If an unknown target 'x' is correlated with filters 'a' and 'b' and the two-filter discrimination ratio

$$D_{xab}^2 \equiv \frac{C_{xb}^n}{C_{xa}^n}$$

is computed, a high value (i.e. $D_{xab}^2 \gg 1$) indicates a high probability the 'x' input is a 'b' target and vice versa. If the input is neither an 'a' nor a 'b', the normalized correlations (numerator and denominator above) are both expected to be much less than one.

Based on the above discussion, a simple "two-filter" recognition strategy based on the defined normalized correlations is as follows:

1. Compute the normalized correlations of an unknown input with 2 or more smart filters representing two or more distinct classes (including possibly different aspects of the same target).

2. If there is no normalized correlation above a specified threshold, then the recognition fails for this input. This threshold must be determined empirically using statistical metrics such as the receiver operating characteristic (ROC) to trade off false alarms versus recognition probability.

3. Otherwise, the filter yielding the greatest normalized correlation recognizes the target. A confidence level may be based on how close the value is to unity and/or how much it exceeds the normalized correlations for the other filters.

Correlation simulations were conducted to determine the (normalized) two-filter discrimination for the M48 and M60 inputs with parametric variations of the azimuthal filter coverage, as previously enumerated. The results are summarized in the following table:

14

Table 4.10 Summary of Normalized Two-filter Discrimination Results for Two Target Types at 135° nominal azimuth

| | Two-filter Discrimination Ratios - dB | | | |
| | M48 Inputs | | M60 Inputs | |
Filter Azimuth Coverage	Average	Worst case	Average	Worst case
4°	4.30	2.70	3.25	1.30
6°	4.13	1.88	2.91	1.46
8°	3.74	1.43	2.61	1.23
12°	3.16	0.93	2.30	1.21

Average values are taken over all available mask inputs falling within the design azimuth coverage of the filter, i.e., varying from about 45 to about 135 inputs. The discrimination ratio was also computed for each individual input and the smallest (least positive) one is given in the "worst case" column.

Similar discrimination results were obtained for broadside (90° nominal azimuth) views. No M60 mask images were available for frontal views, thus preventing discrimination studies at that aspect.

4.4.3 Discussion of Results

The expected degradation of intended-target performance and inter-target discrimination with filter azimuth coverage was not as strong as had been intuitively expected. The most significant degradation occurs in the out-of-band (or ex-band) discrimination ratios, i.e., when the target is the intended target but its azimuth does not match that built into the filter. This is a manifestation of reduced selectivity or reduced azimuth tuning sensitivity. This can be important in a hierarchical filter strategy in which initial correlations with relatively broad filters define azimuth ranges within which finely tuned filters will be applied. The worst-case ex-band discriminations are negative for the 12-degree filters. Based on this, and the slow but definite degradation of all performance measures, including inter-target discrimination, with increased azimuth coverage, 8-degrees of azimuth is the greatest coverage that can be recommended.

5.0 Direct Range Preprocessing

5.1 3D Processing program

A computer program called "opel3d" was written to generate 8-bit height images in row-major format starting with a 'raw' ladar range image, which has 16-bit pixels in column-major format. The program computes height (and horizontal position used to produce an auxiliary plan-view output file) using simple geometric calculations based on known dimensions and the depression (or elevation) angle. Height is output with 1.5" resolution; i.e., the 0-255 pixel value range can cover a height range of 31.88 feet. The horizontal and vertical pixel angular scales are the same as were embodied in the raw range image. For the auxiliary plan-view image, 3" resolution is used for down- and cross-range coordinates. The operator is required to specify several parameters in a configuration file that is read by the program upon execution. These include minimum and maximum range values, elevation, number of rows and columns, and offset and clipping values to map the output heights into a suitable range within the 0-255 range of pixel values. The range limits, offset, and clipping parameters are needed because the overall range of heights that can result from the ladar sensor is much greater than the range spanned by the 8-bit pixels, mentioned above. Some trial-and-error experimentation is required to map the target portion of the image into the desirable range for viewing, i.e., pixel values ranging from 180 to 250.

The auxiliary plan view output file serves to validate the geometric computations; i.e., it should look like the target viewed from overhead.

5.1 Preprocessing for binarization

Two height images generated by opel3d for input file 9762600r.dat (M48 tank at 22° elevation and about 45° azimuth) are shown in the following figure:

Figure 5.1 Height images produced by opel3d computer program. Left is with no median processing. Right is with double median processing

The left image is generated by opel3d with no median processing. Vertical pattern noise, which occurs every seventh column, can be discerned. Several approaches to minimize this noise were tried. The most effective approach was to apply 3x3-sample median processing to the raw range image, repeated for two cycles. This yields the right hand image, in which the pattern noise is eliminated with only a small degradation of image features. The number of median cycles applied is another parameter controlled by the opel3d configuration file.

The following figure contains binary images resulting from applying Sobel and range edge-enhancement operators followed by thresholding, as described in Section 3, to the double-median filtered height image shown above:
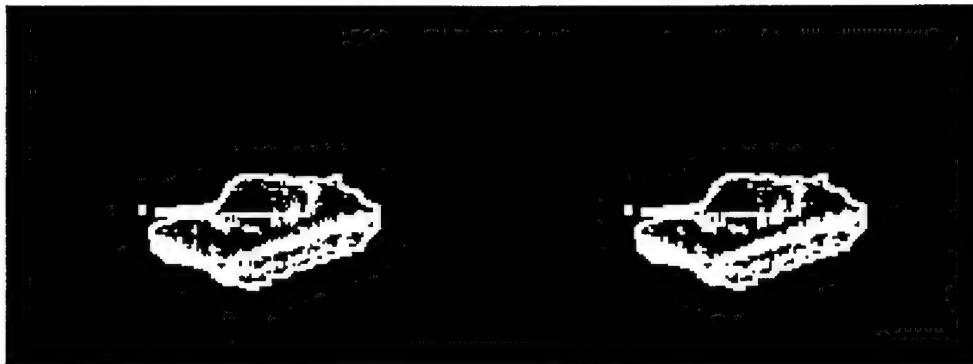

Figure 5.2 Examples of binary images obtained by edge-enhancing and thresholding the double-median processed height image shown in the previous figure. Left image used range operator; right image used Sobel operators.

The binarization threshold used in both cases was 50% of the non-zero pixels. Obviously, these images provide much more internal target detail than the edge image shown on the right side of Figure 3.1. No obvious superiority is apparent for either of the edge enhancement operators; thus the range operator would be preferred because of its smaller computational requirements.

17

6.0 Intensity Calibration Test Set

A practical consideration in relating correlation simulation results, such as those involved in this effort, to experimental correlation results is obtaining a calibration of correlation intensity values. Correlation simulations rarely model the experimental correlator to the degree of fidelity required to accurately predict absolute light intensity values appearing in the correlation plane or, more practically, the captured pixel values. Also, experimental correlators invariably have a noise floor, i.e., a minimum noise level that appears in the output but which is not predicted by simulations. Correlation filters must be designed with sufficient correlation efficiency to provide desired recognition peaks somewhat above this noise floor. The calibration issue is defined by asking "what is this minimum value in terms of correlation simulation intensity 'units' ?"

An image-filter set was defined via simulations to provide a test set for the experimental correlator for the purpose of determining the intensity calibration. The approach taken was to start with a single view M48 tank mask image and the corresponding simple BPOF filter. The correlation for this pair is relatively strong, expected to be perhaps a factor of ten above the noise floor. Then a set of variations of the input image were generated by randomly zeroing a percentage of the pixels, in steps of five percent. Correlation simulations of these images with the single filter provide a smooth progression of peak response intensity over a wide range as shown in the following plot:
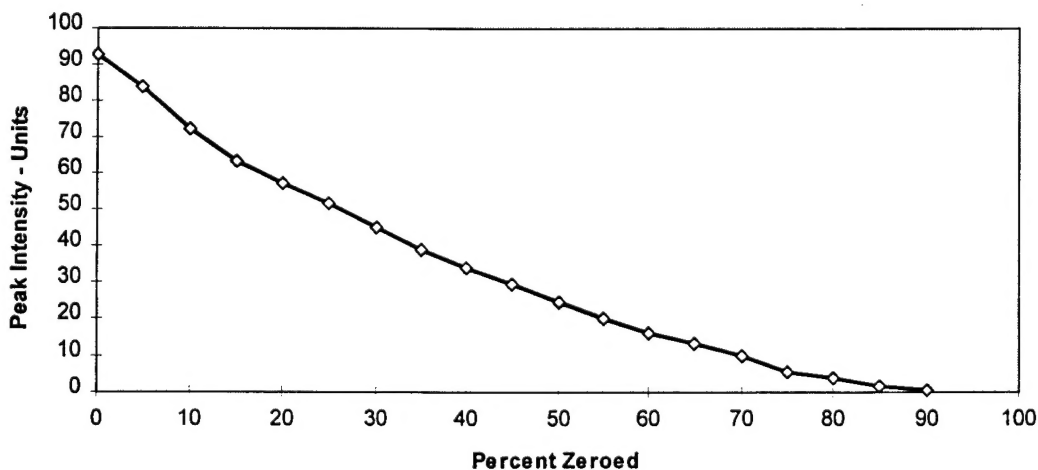

Figure 6.1 Peak Intensity vs. Percent Input Pixels Zeroed. 9762420m mask image - matching BPOF, TLA=30

18

The experimental calibration procedure is to find the input image which provides a correlation peak that is just high enough to be considered detectable (by whatever criterion the user deems appropriate) above the noise floor of the correlator. The simulation peak intensity value (from the ordinate of the above plot corresponding to entering the percent pixels zeroed as the abscissa) defines the minimum peak intensity (filter efficiency) that must be used as a constraint in filter design and simulation testing.

7.0 Conclusions and Recommendations

7.1 Conclusions

The reported design studies have demonstrated in correlation simulations that useful smart filters can be designed based on the provided mask images. The maximum useful azimuth coverage per filter, assuming coverage of the three provided elevations (22°, 25° and 28°), is eight degrees, limited most severely by filter azimuth tuning or selectivity. Nominal aspects of head-on (6° azimuth), rear-quartering (135° azimuth), and broadside (90° azimuth) were included in the studies.

The M48 and M60 targets were successfully discriminated by the designed filters, even with azimuth coverages as large as 12° per filter.

Relatively simple algorithms were developed to generate binary images with good edge and internal detail based on processing of height images derived from the raw ladar range files.

7.2 Recommendation

It is recommended that correlation studies using binary height-based images, as developed in this study, be conducted.

8.0 REFERENCES

1. J. C. Russ, The Image Processing Handbook, CRC Press, Boca Raton, 1992.

2. D. L. Flannery, "Optimal trade off distortion tolerant constrained modulation correlation filters," JOSA-A, Vol. 12, p. 66, January 1995.

3. D. L. Flannery, "Correlation Filter and Preprocessing Algorithms for LCIR Images," UDR-TR-95-23, March 1995

4. D. Flannery, J. Loomis and M. Milkovich, "Design elements of binary phase-only correlation filters," Applied Optics, Vol. 27, p. 4231, 15 October 1988.

5. D.L. Flannery and W.B. Hahn, Jr., "TOPS pattern recognition algorithms and their extension to the IR," Proc. SPIE Vol. 2489, p. 9, Orlando, 18 April 1995.

6. D. Jared and D. Ennis, "Inclusion of filter modulation in synthetic-discriminant function filters," Applied Optics, Vol. 28, p. 232, 15 January 1989.

7. S. D. Lindell, "Summary of the Transfer of Optical Processing to Systems: Optical Pattern Recognition Program, " Proc. SPIE, Vol. 2489, p. 20, Orlando, Florida, 18 April 1995.

DISTRIBUTION
(AFRL-MN-EG-TR-1998-7092)

Defense Technical Information Center 1
8725 John J. Kingman Road, Suite 0944
Ft. Belvoir VA 22060-6218

AFRL/CA-N 1
101 W Eglin Blvd, Suite 105
Eglin AFB FL 32542-5434

AFRL/MNOC-1 (Technical Library) 1
203 W Eglin Blvd, Suite 300
Eglin AFB FL 32542-6843

AFRL/MNGI 7
Dr. D. Goldstein
101 W Eglin Blvd, Suite 280
Eglin AFB FL 32542-6810

AFRL/MNG 2
101 W Eglin Blvd, Suite 268
Eglin AFB FL 32542

Naval Air Weapons Center 1
Attn: Dr. Dave Burdick
Code C2901A
China Lake CA 93555-6001

Comdr, U.S. Army Missile Command 1
Attn: AMSMI-RD-GC-N (Mr. Monte Helton)
Redstone Arsenal AL 35898-5241

IIT Research Institute/GACIAC 1
10 West 35th Street
Chicago IL 60616-3799